

This paper has been downloaded from the Building and Environmental Thermal Systems Research Group at Oklahoma State University (<https://betsrg.org>)

The correct citation for the paper is:

Chiasson, A.C. , S.J. Rees, J.D. Spitler. 2000. A Preliminary Assessment Of The Effects Of Ground-Water Flow On Closed-Loop Ground-Source Heat Pump Systems. ASHRAE Transactions. 106(1): 380-393.

Reprinted by permission from ASHRAE Transactions (Vol. #106 Part 1, pp. 380-393).
© 2000 American Society of Heating, Refrigerating and Air-Conditioning Engineers, Inc.

A Preliminary Assessment of the Effects of Groundwater Flow on Closed-Loop Ground-Source Heat Pump Systems

Andrew D. Chiasson
Student Member ASHRAE

Simon J. Rees, Ph.D.

Jeffrey D. Spitler, Ph.D., P.E.
Member ASHRAE

ABSTRACT

A preliminary study has been made of the effects of groundwater flow on the heat transfer characteristics of vertical closed-loop heat exchangers and the ability of current design and in-situ thermal conductivity measurement techniques to deal with these effects. It is shown that an initial assessment of the significance of groundwater flow can be made by examining the Peclet number of the flow. A finite-element numerical groundwater flow and heat transfer model has been used to simulate the effects of groundwater flow on a single closed-loop heat exchanger in various geologic materials. These simulations show that advection of heat by groundwater flow significantly enhances heat transfer in geologic materials with high hydraulic conductivity, such as sands, gravels, and rocks exhibiting fractures and solution channels. Simulation data were also used to derive effective thermal conductivities with an in-situ thermal conductivity estimation procedure. These data were used to design borehole fields of different depths for a small commercial building. The performance of these borehole field designs was investigated by simulating each borehole field using the pre-calculated building loads over a ten-year period. Results of these simulations, in terms of the minimum and peak loop temperatures, were used to examine the ability of current design methods to produce workable and efficient designs under a range of groundwater flow conditions.

INTRODUCTION

Ground-source heat pump systems have become increasingly popular for both residential and commercial heating and cooling applications because of their higher energy efficiency compared with conventional systems. In closed-loop ground-

source heat pump systems, heat rejection/extraction is accomplished by circulating a heat exchange fluid through high-density polyethylene pipe buried in horizontal trenches or vertical boreholes. The heat exchange fluid is usually water, brine, or an antifreeze solution depending on expected operating conditions. Vertical borehole systems are preferred over horizontal trench systems in applications where the heating and/or cooling load is relatively large because less ground area is required. This paper deals with vertical borehole ground-coupled heat pump systems.

In vertical borehole ground-coupled systems, the ground heat exchanger consists of a number of boreholes, typically 100 ft to 300 ft (30.5 m to 91.4 m) deep with a diameter ranging from 3 in. to 5 in. (76 mm to 127 mm), each containing a U-tube pipe. Typical U-tubes have a diameter in the range of $\frac{3}{4}$ in. to $1\frac{1}{2}$ in. (19 mm to 38 mm). The borehole annulus is generally backfilled with a material that provides thermal contact between the pipe and the soil/rock and prevents cross-contamination of groundwater. In nonresidential ground-coupled systems, the ground loop heat exchanger comprises a borehole field on the order of 10-100 boreholes.

One of the fundamental tasks in the design of a reliable ground-coupled heat pump system is properly sizing the ground loop heat exchanger (i.e., depth of boreholes). Particularly for large systems, an extensive effort is made to design the ground loop heat exchangers so that they are not too large (resulting in a first cost that is too high) or too small (resulting in the system's thermal capacity degrading over time). Several methods and commercially available design software tools exist for this purpose (Ingersoll et al. 1954; Kavanaugh 1984; Eskilson 1987; IGSHPA 1991; Spitler et al. 1996; Kavanaugh and Rafferty 1997). All of these design tools are based on principles of heat conduction and rely on some estimate of the

Andrew D. Chiasson is a research assistant, **Simon J. Rees** is a post-doctoral research associate, and **Jeffrey D. Spitler** is an associate professor in the School of Mechanical and Aerospace Engineering at Oklahoma State University, Stillwater.

ground thermal conductivity and volumetric specific heat. These parameters are perhaps the most critical to the system design, yet adequately determining them is often the most difficult task in the design phase.

Methods of determining the thermal properties of the ground have been the subject of considerable research recently (Mogensen 1983; Eklof and Gehlin 1996; Shonder and Beck 1999; Austin et al. 2000). Current methods range from estimating values from published data to conducting laboratory experiments on soil/rock samples to conducting single-borehole in-situ field tests. In general, thermal property values derived from in-situ field tests are most representative because the values are site-specific and a larger volume of material is evaluated under more realistic conditions than is possible in the laboratory. The typical procedure in in-situ tests is to measure the temperature response of a fluid circulated through a single ground loop heat exchanger with a constant heat flux applied.

Determination of thermal conductivity from in-situ measured temperature-time data is an inverse heat transfer problem. Several methods have been proposed for solving this problem, each of which is based on either an analytical or numerical ground heat transfer model. The analytical heat transfer models used include the “cylinder-source” analytical solution (Carslaw and Jaeger 1946) and the “line-source” analytical solution (Kelvin 1882; Ingersoll et al. 1954). A number of numerical models have been developed (Mei and Emerson 1985; Muraya et al. 1996; Rottmayer et al. 1997). A parameter estimation method using a finite volume numerical model was recently reported by Austin et al. (2000). Each of these methods is based on Fourier’s law of heat conduction and do not take into consideration the effects of groundwater flow.

A further complication in the design of ground-coupled heat pump systems is the presence of groundwater. Where groundwater is present, flow will occur in response to hydraulic gradients, and the physical process affecting heat transfer in the ground is inherently a coupled one of heat diffusion (conduction) and heat advection by moving groundwater. In general, steadily flowing groundwater can be expected to be beneficial to the thermal performance of closed-loop ground heat exchangers. Advection of heat away from the borehole field will alleviate the possible buildup of heat around the boreholes over time.

The presence of flowing groundwater also complicates the borehole field design process. This arises from the fact that both current ground loop heat exchanger design methods and in-situ conductivity measuring methods are based on models that only consider heat conduction. Therefore, there are two ways in which the design process may fail in cases where there is flowing groundwater.

- In-situ measured ground thermal conductivities may appear artificially high.
- Borehole fields designed using the measured, artificially high thermal conductivities may be over- or under-designed.

It is clear that under in-situ test conditions the groundwater flow will result in smaller temperature differences for given heat input, as some heat is carried away by the groundwater. Hence, derived thermal conductivities will always appear higher. Unusually high thermal conductivity values were recently reported from in-situ test data at a site in Minnesota, where there was believed to be significant groundwater flow (Remund 1998). The presence of groundwater flow changes the heat transfer problem from one of purely heat conduction to one of coupled flow and advective-diffusive heat transfer. Consequently, it is not immediately clear whether borehole fields designed using in-situ test data derived under these conditions will be over- or under-designed.

The objectives of this work have been to make a preliminary examination of the effects of groundwater flow on both in-situ conductivity measurements and long-term borehole field performance. This has been attempted by first examining the range of hydrogeological conditions that might be expected and estimating the order of magnitude of the corresponding groundwater flows. A simple method of examining the importance of heat advection from groundwater flow is then presented.

A finite-element numerical groundwater flow and heat transport model has been used to simulate and observe the effects of groundwater flow on the average fluid temperature in a single U-tube borehole in various geologic materials. This model was used to simulate several in-situ thermal conductivity tests, and thermal conductivities were derived from these data using standard in-situ test procedures. For each test case, the derived thermal conductivities, along with the thermal loads from an actual building, were used to design a hypothetical borehole field by employing conventional design tools and procedures. For each set of hydrogeological conditions, a numerical model of the whole borehole field was used to simulate its long-term performance. Conclusions are presented on the ability of conventional design procedures to correctly predict the long-term performance of closed-loop ground heat exchangers under different groundwater flow conditions.

COUPLED GROUNDWATER FLOW AND HEAT TRANSPORT

Groundwater Flow

Undergroundwater occurs in two zones: the unsaturated zone and the saturated zone. The term “groundwater” refers to water in the saturated zone. The surface separating the saturated zone from the unsaturated zone is known as the “water table.” At the water table, water in soil or rock pore spaces is at atmospheric pressure. In the saturated zone (below the water table), pores are fully saturated and water exists at pressures greater than atmospheric. In the unsaturated zone, pores are only partially saturated and the water exists under tension at pressures less than atmospheric. In this paper, we deal only with water in the saturated zone.

Groundwater is present nearly everywhere, but it is only where the local geology results in the formation of aquifers that significant flows of groundwater can be expected. Driscoll (1986) defines an aquifer as a “formation, group of formations, or part of a formation that contains sufficient saturated permeable material to yield economical quantities of water to wells and springs.” Aquifers are described as being either confined or unconfined. Confined aquifers are bounded between two or more layers of rock (or clay soils) of low permeability. Unconfined aquifers are bounded at their upper surface by the water table. In practice, the boreholes of ground loop heat exchangers may partially penetrate unconfined aquifers and/or at greater depths penetrate into confined aquifers.

The governing equation describing flow through porous media is Darcy’s law. This is commonly used to model the flow in the saturated zone of groundwater systems and can be expressed as

$$q = -K \frac{dh}{dx} \quad (1)$$

where q is the specific discharge (volume flow rate per unit of cross-sectional area), K is the hydraulic conductivity, and h is the hydraulic head. The specific discharge is related to the average linear velocity, v , by $v = q/n$, where n is the porosity and is introduced to account for the difference between the unit cross-sectional area and the area of the pore spaces through which the groundwater flows (Freeze and Cherry 1979; Fetter 1988).

By applying the law of conservation of mass to a control volume and making use of Darcy’s law (Equation 1), an equation defining the hydraulic head distribution can be derived. Transient groundwater flow with constant density can then be expressed in cartesian tensor notation as

$$S_s \frac{\partial h}{\partial t} - \frac{\partial}{\partial x_i} \left(K_{ij} \frac{\partial h}{\partial x_j} \right) = R^* \quad (2)$$

Heat Transport in Groundwater

Heat can be transported through a saturated porous medium by the following three processes:

1. Heat transfer through the solid phase by conduction.
2. Heat transfer through the liquid phase by conduction.
3. Heat transfer through the liquid phase by advection.

The governing equation describing heat transport in the ground with flowing groundwater is a partial differential equation of the advection-dispersion¹ type (Freeze and Cherry 1979). By applying the law of conservation of energy to a control volume, an equation for heat transport can be found and expressed as

$$nR \frac{\partial T}{\partial t} + v_i \frac{\partial T}{\partial x_i} - \frac{\partial}{\partial x_i} \left(D_{ij} \frac{\partial T}{\partial x_j} \right) = Q^* \quad (3)$$

where the velocity, v_i , is determined from the solution of Equation 2, and T is the temperature of the rock/water matrix. It is the second term in this equation that represents advection of heat by the groundwater and couples Equations 2 and 3 together. If the groundwater velocity is zero, Equation 3 reduces to a form of Fourier’s law of heat conduction.

The diffusion coefficient tensor D_{ij} is modeled here as an effective thermal diffusivity given by

$$D^* = \frac{k_{eff}}{\rho_l c_l} \quad (4)$$

The effective thermal conductivity, k_{eff} , is a volume weighted average thermal conductivity of the saturated water/rock matrix and can be expressed using the porosity as

$$k_{eff} = nk_l + (1-n)k_s \quad (5)$$

It is necessary to distinguish between the conductivity and thermal capacity of the water and rock in this way to account for the fact that heat is stored and conducted through both the water and rock, but heat is only advected by the water. Similarly, it is necessary to define a retardation coefficient R , which multiplies the temporal term of Equation 3 (Bear 1972). This is given by

$$R = \frac{1 + (1-n)c_s \rho_s}{nc_l \rho_l} \quad (6)$$

Typical Hydraulic and Thermal Property Values for Soils and Rocks

In assessing the significance of groundwater flow to closed-loop heat exchanger performance, the question arises in what locations will groundwater flow be significant. Darcy’s law (Equation 1) indicates that flow is dependent on both the local hydraulic gradient and the hydraulic conductivity of the local geologic material. Heat transfer is dependent on the flow and thermal conductivity (Equation 3). It is therefore useful, in making a preliminary assessment of the significance of groundwater flow, to consider the range of naturally occurring soil and rock properties and possible values of hydraulic gradient.

Naturally occurring ranges of values of hydraulic and thermal properties of soils and rocks are summarized in Table 1. Values of hydraulic gradient are somewhat more site-specific; the United States Environmental Protection Agency (1996) reports a typical range of hydraulic gradient values of 0.0001 to 0.05.

Some specific examples of natural groundwater velocities include: 1796 ft/yr to 7185 ft/yr (547.5 m/yr to 2190 m/yr) under a hydraulic gradient of 0.002 to 0.012 in the Snake River Group basalt, Idaho, USA (Lindholm and Vaccaro 1988); 361 ft/yr (110 m/yr) in the High Plains sand and

¹ This type of equation is also referred to as a convection-diffusion equation. We use the term “advection” here rather than “convection” to prevent any confusion with use of “convection” to describe surface-to-fluid heat transfer.

TABLE 1
Typical Values of Hydraulic and Thermal Properties of Soils and Rocks

Porous Medium	Hydraulic Properties					Thermal Properties			
	Hydraulic Conductivity [†] (K) ft/s (m/s)		Porosity [†] (n) (--)		Velocity [‡] (v) ft/yr (m/yr)	Thermal Conductivity ^{††} (k) Btu/h·ft·°F (W/m·°C)	Volumetric Heat Capacity ^{††} ($\rho_s c_s$) Btu/ft ³ ·°F (J/m ³ ·°C)		
	Range	Geometric Average	Range	Arithmetic Average		Range	Arithmetic Average	Range	Arithmetic Average
Soils									
Gravel	9.84E-04 - 9.84E-02 3.00E-04 - 3.00E-02	9.84E-03 3.00E-03	0.24 - 0.38	0.31	1.00E+04 3.05E+03	0.40 - 0.52 (0.70) - (0.90)	0.46 (0.80)	-- --	2.09E+01 (1.40E+06)
Sand (coarse)	3.0E-06 - 2.0E-02 (9.0E-07) - (6.0E-03)	2.4E-04 (7.3E-05)	0.31 - 0.46	0.385	1.98E+02 (6.01E+01)	0.40 - 0.52 (0.70) - (0.90)	0.46 (0.80)	-- --	2.09E+01 (1.40E+06)
Sand (fine)	6.6E-07 - 6.6E-04 (2.0E-07) - (2.0E-04)	2.1E-05 (6.3E-06)	0.26 - 0.53	0.40	1.66E+01 (5.05E+00)	0.40 - 0.52 (0.70) - (0.90)	0.46 (0.80)	-- --	2.09E+01 (1.40E+06)
Silt	3.3E-09 - 6.6E-05 (1.0E-09) - (2.0E-05)	4.6E-07 (1.4E-07)	0.34 - 0.61	0.475	3.08E-01 (9.40E-02)	0.69 - 1.39 (1.20) - (2.40)	1.04 (1.80)	3.58E+01 - 4.92E+01 (2.40E+06) - (3.30E+06)	4.25E+01 (2.85E+06)
Clay	3.3E-11 - 1.5E-08 (1.0E-11) - (4.7E-09)	7.1E-10 (2.2E-10)	0.34 - 0.60	0.47	4.78E-04 (1.46E-04)	0.49 - 0.64 (0.85) - (1.10)	0.56 (0.98)	4.47E+01 - 5.37E+01 (3.00E+06) - (3.60E+06)	4.92E+01 (3.3E+06)
Rocks									
Limestone, dolomite	3.3E-09 - 2.0E-05 (1.0E-09) - (6.0E-06)	2.5E-07 (7.7E-08)	0 - 0.20	0.10	8.02E-01 (2.44E-01)	0.87 - 1.91 (1.50) - (3.30)	1.39 (2.40)	3.17E+02 - 8.20E+01 (2.13E+07) - (5.50E+06)	1.99E+02 (1.34E+07)
Karst limestone	3.3E-06 - 3.3E-02 (1.0E-06) - (1.0E-02)	3.3E-04 (1.0E-04)	0.05 - 0.50	0.275	3.76E+02 (1.15E+02)	1.44 - 2.48 (2.50) - (4.30)	1.96 (3.40)	3.17E+02 - 8.20E+01 (2.13E+07) - (5.50E+06)	1.99E+02 (1.34E+07)
Sandstone	9.8E-10 - 2.0E-05 (3.0E-10) - (6.0E-06)	1.4E-07 (4.2E-08)	0.05 - 0.30	0.18	2.51E-01 (7.65E-02)	1.33 - 3.76 (2.30) - (6.50)	2.54 (4.40)	3.17E+01 - 7.46E+01 (2.13E+06) - (5.00E+06)	5.31E+01 (3.56E+06)
Shale	3.3E-13 - 6.6E-09 (1.0E-13) - (2.0E-09)	4.6E-11 (1.4E-11)	0 - 0.10	0.0525	2.79E-04 (8.50E-05)	0.87 - 2.02 (1.50) - (3.50)	1.44 (2.50)	3.54E+01 - 8.20E+01 (2.38E+06) - (5.50E+06)	5.87E+01 (3.94E+06)
Fractured igneous and metamorphic	2.6E-08 - 9.8E-04 (8.0E-09) - (3.0E-04)	5.1E-06 (1.5E-06)	0 - 0.10	0.05	3.21E+01 (9.78E+00)	1.47 - 3.83 (2.50) - (6.60)	2.65 (4.58)	-- --	3.28E+01 (2.20E+06)
Unfractured igneous and metamorphic	9.8E-14 - 6.6E-10 (3.0E-13) - (2.0E-10)	8.0E-12 (2.4E-12)	0 - 0.05	0.025	1.01E-04 (3.09E-05)	1.47 - 3.83 (2.50) - (6.60)	2.65 (4.58)	-- --	3.28E+01 (2.20E+06)

Notes: Thermal conductivity values are taken to represent those of materials in the dry condition.

[†] Hydraulic conductivity and porosity data from Domenico and Schwartz (1990).

[‡] v is the average linear groundwater velocity based on an assumed gradient of 0.01 ft/ft (m/m).

^{††} Thermal property data from Hellstrom (1991). For sedimentary rocks, Hellstrom lists only c_s . In these cases, a density of 2500 kg/m³ is assumed.

gravel aquifer, western central USA (Weeks and Gutentag 1988); and 1.3×10^{-3} ft/yr to 1.50×10^{-2} ft/yr (4.0×10^{-4} m/yr to 4.6×10^{-3} m/yr) in glacial clay soils in Southern Ontario, Canada (Stephenson et al. 1988). Local pumping activities may further increase groundwater flow rates in aquifers.

The thermal properties of soils and rocks are functions of mineral content, porosity, and degree of saturation. Of these, porosity may be considered the most important property simply because of the origin and nature of soils and rocks. Rocks originate under higher heat and pressure environments than soils and, consequently, generally possess lower porosities. Lower porosities in rocks result in higher contact area between grains and, therefore, higher thermal conductivities than soils, regardless of mineral content. For saturated materials, increased porosity results in increased heat capacities and, therefore, lower thermal diffusivities.

The porosity of soils and rocks can also be an important controlling influence on hydraulic conductivity (Freeze and Cherry 1979). Materials with higher porosity generally also have higher hydraulic conductivity. However, this correlation does not hold for fine-grained soils (see Table 1). Porosity and hydraulic conductivity of soils and rocks can be increased by so-called "secondary porosity," which is attributed to solution channels (e.g., in karst limestone) or to fracturing (e.g., in rocks and cohesive soils).

Conduction vs. Advection in Geologic Materials

It has already been noted that it is the presence of advection that distinguishes the heat transfer regime under groundwater flow conditions from that of heat conduction alone. Some assessment of the significance of the flow can be made by considering the order of magnitude of the advection of heat compared to conduction (diffusion).

The dimensionless parameter describing conduction vs. convection is Pe, the Peclet number. In this application the Peclet number expresses the transport of heat by bulk fluid motion to the heat transported by conduction. Domenico and Schwartz (1990) define Pe for heat transport in groundwater as

$$Pe = \rho_i c_i q L / K_{eff} \quad (7)$$

The term L is a characteristic length dependent on the type of problem. According to Bear (1972), L can be chosen as any length dimension, so long as it is consistent with other comparisons. In principle, advection becomes significant when the Peclet number is of order one. The exact value of Pe at which advection becomes significant is slightly dependent on the choice of L .

The Peclet number has often been used to quantify the relative importance of advection vs. molecular diffusion when discussing mass transport in groundwater. Bear (1972) summarizes the data from many of the studies that have been conducted. In short, when the characteristic length was chosen as mean grain size, diffusion is the process dominating mass transport at Peclet numbers less than about 0.4. At Peclet

numbers in the range of 0.4 to 5, a transition occurs where advection (or mechanical dispersion) and diffusion are of the same order of magnitude. Above a Peclet number of about 5, advection was found to dominate. The authors know of no similar studies conducted for heat transport in groundwater flows.

An analysis of the Peclet number using the typical hydraulic and thermal values of soils and rocks presented in Table 1 may be used to assess the role of groundwater flow in the design of closed-loop ground heat exchangers. The characteristic length could conceivably be chosen as (1) typical borehole spacing or (2) the length of the borehole field in the direction of flow. Here we have chosen to use a borehole spacing of 14.8 ft (4.5 m). The groundwater property values of ρ_f , c_f , and k_f were taken as 62.4 lb/ft³ (1000 kg/m³), 1.0 Btu/lb·°F (4180 J/kg·K), and 0.347 Btu/h·ft·°F (0.60 W/m·K). The calculated Peclet numbers are listed in Table 2.

A review of the data presented in Table 2 reveals that heat advection by groundwater flow is a significant process contributing to heat transfer in coarse-grained soils (sands and

TABLE 2
Peclet Numbers Corresponding to Typical Values of Hydraulic and Thermal Properties of Soils and Rocks

Porous Medium	Peclet Number where $L = a$ typical borehole spacing of 14.8 ft (4.5 m) [--]
Soils	
Gravel	5.72E+02
Sand (coarse)	1.34E+01
Sand (fine)	1.15E+00
Silt	1.28E-02
Clay	3.24E-05
Rocks	
Limestone, dolomite	5.92E-03
Karst limestone	5.28E+00
Sandstone	1.77E-03
Shale	1.05E-06
Fractured igneous and metamorphic	6.32E-02
Unfractured igneous and metamorphic	1.00E-07

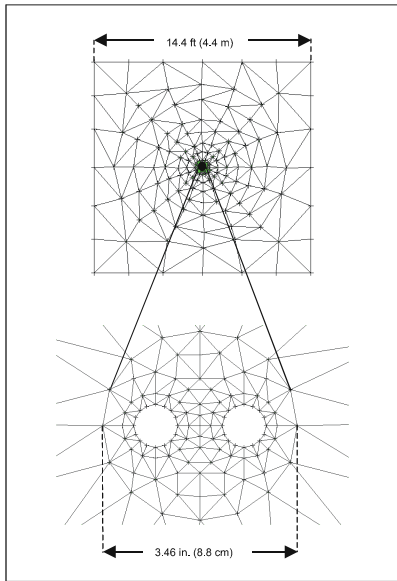


Figure 1 The finite element mesh used to represent a single borehole.

gravels) and in rocks exhibiting secondary porosities (fracturing and solution channels). When the characteristic length is defined as the borehole spacing, Peclet numbers exceeding 1 exist only for sands, gravels, and karst limestones. It is possible, however, that even where the Peclet number is of order one or higher, the effects of the groundwater flow on the temperature response may not be seen within the normal time scale of an in-situ conductivity test. This is one of the reasons for conducting numerical borehole field simulations of several years' duration.

THE NUMERICAL MODEL

A finite element groundwater flow and mass/heat transport model has been used in this work as the primary means of assessing the effects of groundwater flow. Use of a numerical model allows a wide range of conditions to be examined and is the only practical means of modeling an entire borehole field. In each test case a unidirectional flow field was imposed over the whole numerical domain. As the flow was assumed to be fully saturated, and within homogeneous geological material, it was only necessary to use a two-dimensional model.

In the numerical model used here, the governing partial differential Equations 2 and 3 are discretized spatially by a Galerkin finite element method using triangular elements with linear weighting functions (Vatnaskil 1998). The temporal term of the equations is dealt with by first order backward differencing in time. The finite element method as implemented in the commercial code used here (Vatnaskil 1998) does not allow the explicit representation of the heat transport equation but provides a general form of the mass transport equation. This equation is analogous to the heat transport

equation (Equation 3). Temperatures were, in fact, calculated by suitable choice of the coefficients of the mass transport equation and corresponding adaptation of the boundary conditions.

The Finite Element Mesh

Finite element meshes for a single borehole geometry and for a complete borehole field geometry have been constructed using triangular elements. Nodal spacing was kept relatively fine around the pipe walls where the largest temperature gradients were expected. The mesh for the single borehole geometry was constructed within a square domain and consisted of 465 nodes, as shown in Figure 1.

A mesh for a four-by-four configuration borehole field was constructed using the single borehole mesh (Figure 1) as the basis for the mesh at each borehole and expanding the mesh in the direction of groundwater flow, as shown in Figure 2. This mesh consisted of 4532 nodes.

Boundary Conditions

Two sets of boundary conditions are required: one set for the flow model and one set for the transport model. In the flow model, Dirichlet (fixed value) boundary conditions were set on the left- and right-hand boundaries in order to impose a fixed hydraulic gradient. Neumann (fixed gradient) boundary conditions were set on the upper and lower boundaries of the flow domain and are specified as zero flux. We assume that no recharge takes place across the water table within the model domain. In the transport model Dirichlet boundary conditions were set on all four sides of the model domain. These conditions represent fixed background or far-field temperatures.

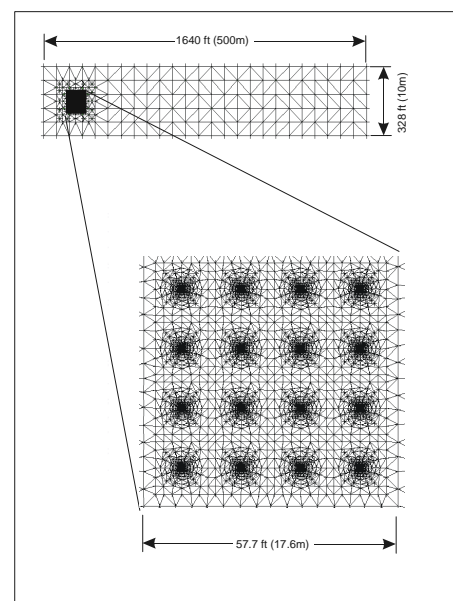


Figure 2 The finite element mesh used to represent a 16 borehole field.

In order to impose the borehole heat loads as boundary conditions at the borehole pipe walls, some adaptation of the usual boundary conditions was required. This arises from the use of the mass transport equation to model heat transport. First, a zero flux condition for the mass (heat) transport equation was applied at each of the 16 nodes forming each pipe wall. The required heat flux is, in fact, imposed by using a source term in the groundwater flow equation at these nodes (representing injection of warm/cold water). The flow injected, V^* , was negligibly small (3.53×10^{-19} ft³/s [1.0×10^{-20} m³/s]) so that the overall flow pattern was not disturbed. The temperature of this injection flow, T_w , was set to achieve the required heat input, so that

$$T_w \approx \frac{q^*}{\rho_l c_l V^*}. \quad (8)$$

The values of ρ_l and c_l are taken as constants of 62.4 lb/ft³ (1000 kg/m³) and 1.0 Btu/lb·°F (4180 J/kg·K). For the purposes of output, the average temperature of the heat exchange fluid in each borehole is taken as the average of the nodal temperatures of the 32 nodes defining the U-tube pipe in each borehole. Where single borehole cases were simulated, the heat input per pipe node, q^* , was set at a fixed value representative of in-situ test conditions. Where the whole borehole field was modeled, this was determined from the time varying building loads.

RESULTS AND DISCUSSION

Single-Borehole Simulations

The numerical model was initially used to make calculations of average borehole temperatures for a range of soil and rock types over a two-year simulation time. The objective was to examine the trends in heat exchanger performance with increasing Peclet number. For each calculation a hydraulic gradient of 0.01 was applied and the hydraulic conductivity set as given in Table 1. A constant heat flux of 8530 Btu/h (2500 W) was applied on a U-tube in a 250 ft (76.2 m) deep borehole. The initial temperature was set at 63°F (17.2°C). The model domain is that shown in Figure 1. For comparison purposes, similar calculations were made for each case but with zero groundwater flow.

The calculated trends in average borehole fluid temperature vs. time for three example geologic materials are shown in Figure 3. A review of these plots reveals that a “typical” groundwater flow rate in coarse sand dramatically lowers the average borehole fluid temperature within a short time when compared to the zero groundwater flow case. After a one-year period, the average fluid temperature in the borehole is approximately 15°F (8.3°C) lower than the average fluid temperature in the borehole where no groundwater flow was simulated and appears to have reached a steady state. A small reduction in peak temperature is shown for the case of fine sand. However, “typical” groundwater flow rates in materials

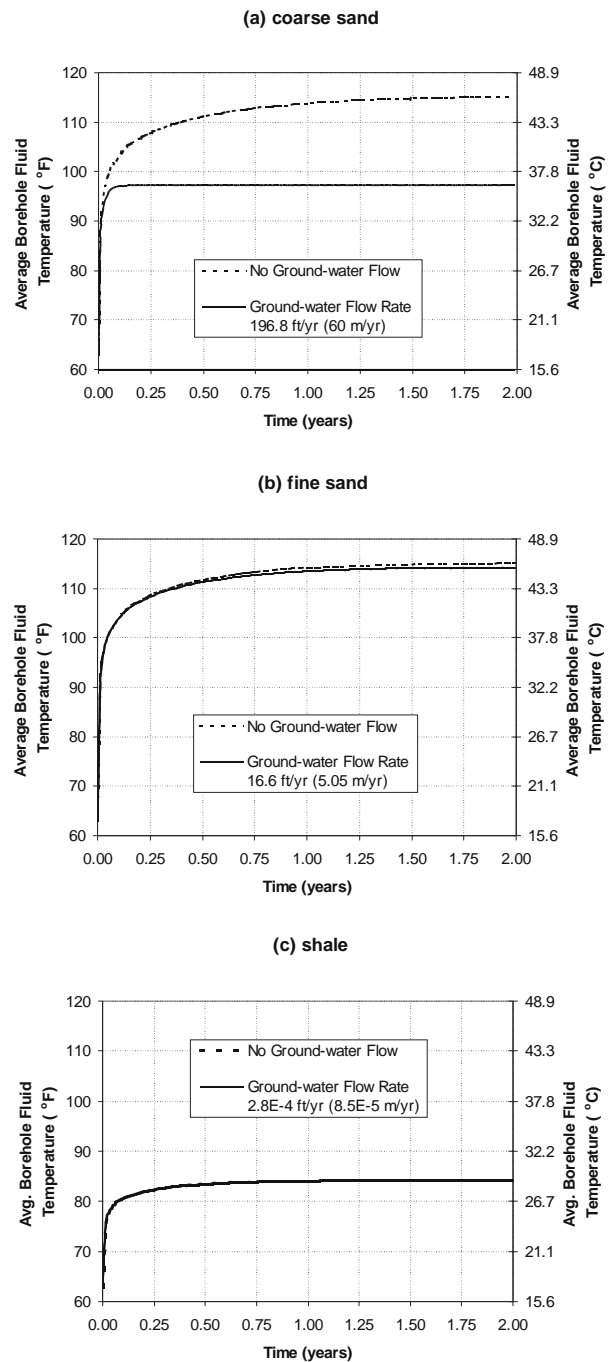


Figure 3 Average borehole fluid temperature vs. time for (a) coarse sand, (b) fine sand, and (c) shale showing the effect of groundwater flow over a two-year period.

such as limestones, dolomites, and shales were found to have negligible effect on the average borehole fluid temperature.

The trends shown in these results are in agreement with the previous Peclet number analysis. At Peclet numbers of order one or higher, advection of heat by flowing groundwater is a significant process contributing to heat transfer in the

ground. At Peclet numbers of order less than one, conduction is the dominant heat transfer process, and the enhancement to the heat exchanger performance is negligible.

Simulated In-Situ Thermal Conductivity Tests

The second objective of the single-borehole simulations was to determine the effects of groundwater flow (in a material where groundwater flow is expected to be significant) on the results of in-situ ground thermal conductivity tests. The previous results showed the effects of groundwater flow to be most significant in the cases of gravel and coarse sand. Accordingly, the simulated in-situ thermal conductivity tests calculations have been based on coarse sand properties.

In in-situ thermal conductivity tests, a steady heat flux is applied to a test borehole and the response in the mean water temperature is measured. These data are used either with an analytical model, or with a numerical model and parameter estimation technique, to arrive at a value of soil thermal conductivity. Here we have calculated borehole temperature response for a range of groundwater flows using the finite element groundwater flow and heat transfer model. These data have then been analyzed using the parameter estimation technique developed by Austin et al. (2000) in exactly the same way as if the data had been measured in-situ. Hence “effective” thermal conductivities have been estimated for different flow conditions.

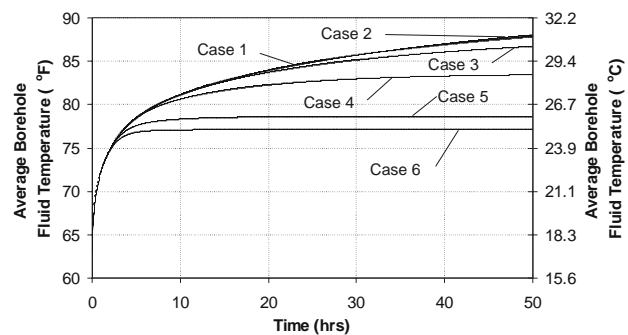
In-situ test conditions were modeled by applying a constant heat flux of 8530 Btu/h (2500 W) to the finite element model of a U-tube in a 250 ft (76.2 m) deep borehole. The typical duration of in-situ ground thermal conductivity tests for the method used here is 50 hours. Simulations were run for this period using a time step of 2.5 minutes. As the effects of groundwater flow were expected to become more apparent with time, further sets of data were generated with simulations of one-week duration. The initial temperature was set at 63°F (17.2°C), and the model domain is that shown in Figure 1. Model input hydraulic and thermal property values are those listed in Table 1 for a coarse sand, except the groundwater flow velocity was varied from a “typical” value of 196.8 ft/yr (60 m/yr) to a more extreme value of 1968.5 ft/yr (600 m/yr) by adjusting the hydraulic conductivity value. Twelve cases were simulated as listed in Table 3.

Resulting temperature responses for the 12 cases are plotted in Figure 4. A review of Figure 4 shows that groundwater flow in coarse sand significantly impacts the average borehole fluid temperature over the time scales of an in-situ ground thermal conductivity test. Two noteworthy conclusions can be drawn from these simulations: (1) as groundwater velocity increases, the time to reach steady-state conditions decreases, and (2) as groundwater velocity increases, the steady-state temperature decreases. Also the deviation from the zero flow condition can be seen to be dependent on the duration of the

TABLE 3
Summary of Simulated In-Situ Ground Thermal Conductivity Test Conditions

Case	Simulation Time Period	Groundwater Flow Velocity
1	50 hours	No groundwater flow
2	50 hours	196.8 ft/yr (60 m/yr)
3	50 hours	393.7 ft/yr (120 m/yr)
4	50 hours	787.4 ft/yr (240 m/yr)
5	50 hours	1574.8 ft/yr (480 m/yr)
6	50 hours	1968.5 ft/yr (600 m/yr)
7	1 week	No groundwater flow
8	1 week	196.8 ft/yr (60 m/yr)
9	1 week	393.7 ft/yr (120 m/yr)
10	1 week	787.4 ft/yr (240 m/yr)
11	1 week	1574.8 ft/yr (480 m/yr)
12	1 week	1968.5 ft/yr (600 m/yr)

(a)



(b)

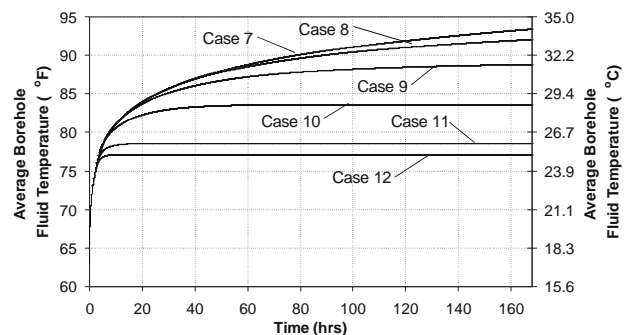


Figure 4 Average borehole fluid temperatures for the 12 simulated in-situ ground thermal conductivity test cases in a coarse sand with groundwater velocities ranging from 0 to 1968 ft/yr (600 m/yr) for (a) 50 hours and (b) one week.

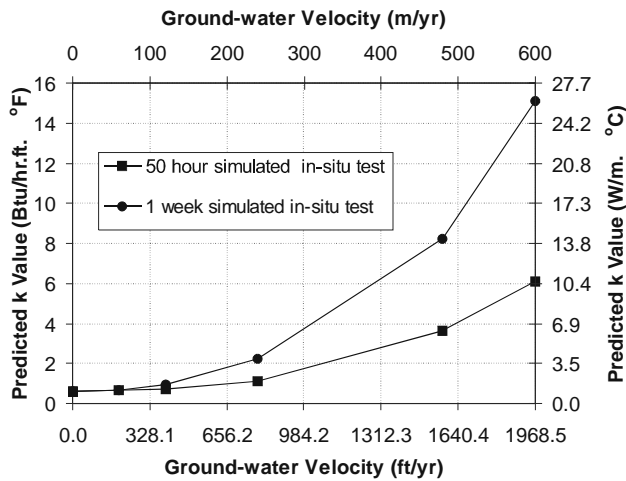


Figure 5 Predicted effective ground thermal conductivity values vs. groundwater flow velocity for 50-hour and one-week simulated in-situ thermal conductivity tests.

test – temperatures are further reduced with increasing duration. Hence, the duration of the test could be expected to have an influence on the estimated thermal conductivity in an in-situ test.

The effective thermal conductivity values predicted by the Austin et al. (2000) model are plotted against the corresponding groundwater flow velocity for each of the two in-situ test simulation times (50 hours and one week) in Figure 5. The estimated thermal conductivity values are listed by case number (as defined in Table 4). A review of these results shows that as groundwater flow velocity increases, the predicted effective thermal conductivity values from a conduction-based model are significantly different, depending on the duration of simulated test. These values are “effective” values and not the true thermal conductivity of the formation since they include the effects of groundwater advection. However, without further analysis, it is not clear if the 50-hour data set or the one-week data set produce values that can be further used in the design process.

Borehole Field Simulations

In order to investigate the effects of groundwater flow on borehole field performance and system design procedures further, the predicted ground thermal conductivities have been used to design a borehole field for a test building. The test building used for designing the borehole field was an actual building located in north-central Oklahoma. This building is a single-story office building with eight thermal zones and has a predominant demand for cooling. The hourly building loads

TABLE 4
Summary of Borehole Field Design Parameters

Case Number	Simulation Duration (hours)	Groundwater Flow Rate ft/yr (m/yr)	Estimated Thermal Conductivity (Austin et al. 2000) Btu/h-ft-°F (W/m-K)	Design Borehole Depth (Spitler et al. 1996) ft (m)
1	50	0	0.643 (1.11)	239.98 (73.15)
2	50	196.85 (60.00)	0.650 (1.12)	238.56 (72.71)
3	50	393.70 (120.00)	0.731 (1.26)	224.10 (68.31)
4	50	787.40 (240.00)	1.146 (1.98)	171.56 (52.29)
5	50	1574.80 (480.00)	3.657 (6.33)	87.24 (26.59)
6	50	1968.50 (600.00)	6.074 (10.51)	61.58 (18.77)
7	168	0	0.625 (1.08)	243.86 (74.33)
8	168	196.85 (60.00)	0.691 (1.20)	230.86 (70.37)
9	168	393.70 (120.00)	0.962 (1.66)	191.58 (58.39)
10	168	787.40 (240.00)	2.250 (3.89)	115.91 (35.33)
11	168	1574.80 (480.00)	8.229 (14.24)	48.02 (14.64)
12	168	1968.50 (600.00)	15.107 (26.14)	26.90 (8.20)

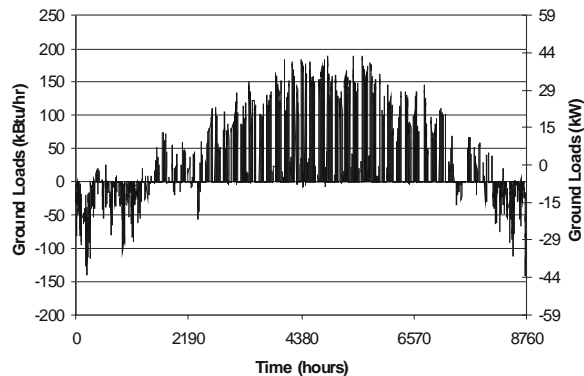


Figure 6 Hourly ground loads for the test building. Heating load is shown negative, representing heat extracted from the ground; cooling load is positive, representing heat rejected to the ground.

were determined for one year using building energy simulation software (BLAST 1986). The building loads were then converted to ground loads under the assumption that all heat pumps in the system have a constant coefficient of performance of 4.0. The ground loads for this building are shown in Figure 6.

Borehole field designs were produced for each of the 12 test cases. This was done using a commercially available ground-loop heat exchanger design software tool (Spitler et al. 1996). A 16 borehole field (four-by-four boreholes in a square pattern) was found adequate for the test building ground loads (Figure 6). The monthly loads and peak hourly loads are input in the design software. For this study, no peak hourly loads were specified for the sake of the computational time required for the subsequent borehole field simulations (see discussion below). Peak design entering fluid temperatures to the heat pump were specified at 90°F (32.2°C) maximum and 35°F (1.7°C) minimum. The borehole depths were sized for 20 years of operation.

For each test case, the corresponding effective thermal conductivity shown in Figure 5 was input into the ground-loop heat exchanger design software. The borehole depths predicted by the design software are plotted against the corresponding groundwater flow velocity for each of the two in-situ test simulation times (50 hours and one week) in Figure 7. The design borehole depths are also listed in Table 4.

The finite element groundwater flow and heat transport model was further used to simulate the long-term performance of each borehole field designed from the simulated in-situ ground thermal conductivity test cases. The model domain was that previously described for the multi-borehole field simulations and is shown in Figure 2. The total simulation time for all cases was ten years using a time step of five days. The simulated heat flux at the internal boundary nodes defining the U-tube pipes was a time varying source corresponding to the

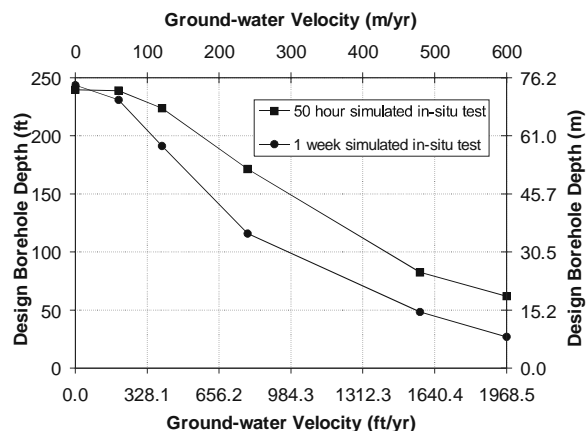


Figure 7 Design borehole depths vs. groundwater velocity for a 50-hour and a one-week simulated in-situ thermal conductivity test.

monthly ground loads for the test building. Hydraulic and thermal property parameters for each borehole field case number were the same as the corresponding single-borehole case number, except for the borehole depths, which are listed in Table 4. Each ten-year simulation required approximately 60 hours of computation time on a personal computer with a 233 MHz processor.

Annual maximum and minimum peak temperatures are plotted for each case in Figure 8. Examination of the cases with no groundwater flow (cases 1 and 7) shows annual rises in peak temperature typical of cooling dominated buildings. After the second year, all of the cases with groundwater flow show minimum and maximum temperatures unchanging from year to year.

Some notable differences can be seen between the borehole field designs based on 50-hour test data compared to one-week test data. This is shown by cases 5 and 6, which used thermal conductivity values determined from a 50-hour test at groundwater flow velocities of 1574.8 ft/yr (480 m/yr) and 1968.5 ft/yr (600 m/yr), respectively, and by cases 11 and 12, which are for the same flow rates but based on thermal conductivities determined from one-week test data. The thermal conductivity values determined in cases 11 and 12 are unrealistically high and, consequently, the design borehole depths are too shallow; the result is that the maximum peak temperature of the simulated borehole field in both cases exceeds the maximum design temperature during the first year. This implies that for in-situ test cases where the average borehole fluid temperature reaches steady state in a short time (as demonstrated by case 4/10, case 5/11, and case 6/12 in Figure 4), increasing the duration of the test results in decreased confidence in the accuracy of the effective thermal conductivity value determined from the test.

Except for cases 11 and 12, the annual maximum and minimum temperatures fell within the design conditions. Having followed conventional design procedures, it is inter-

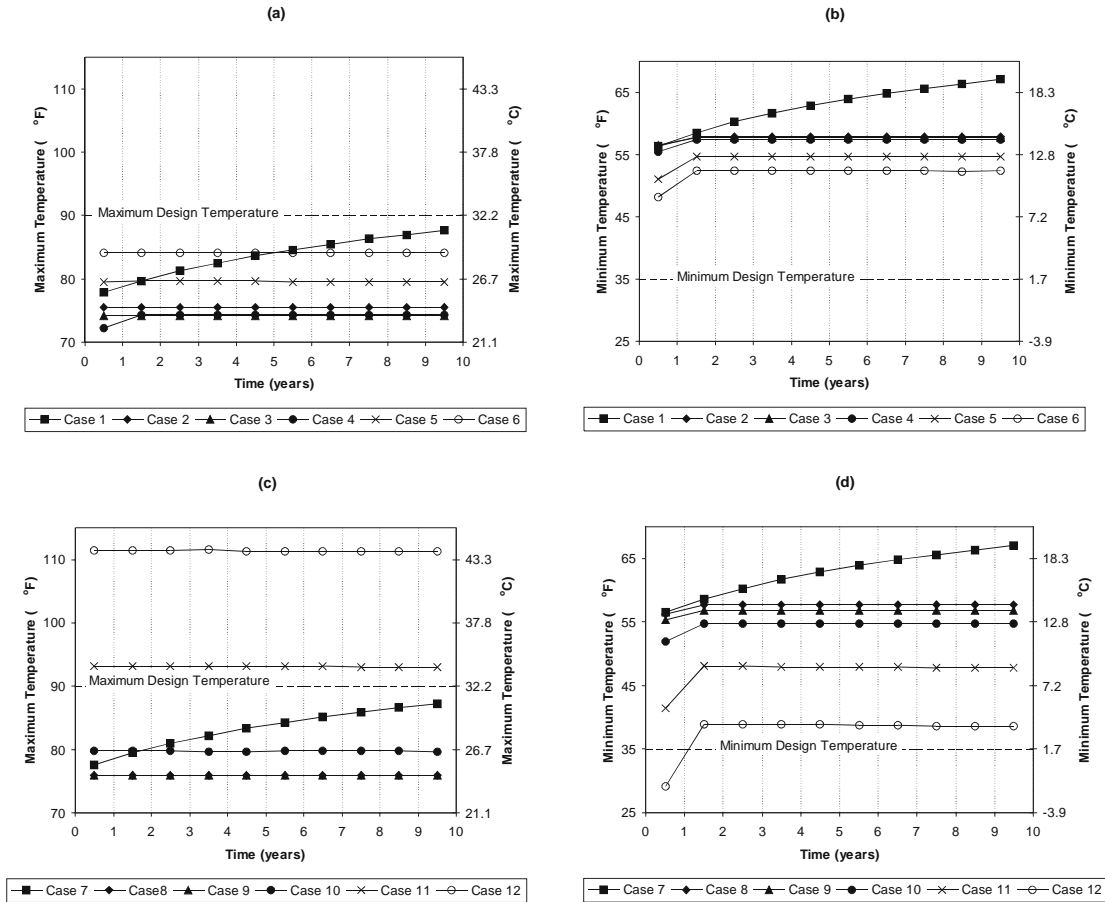


Figure 8 Annual maximum (a and c) and minimum (b and d) average borehole fluid temperatures for the 16-borehole field simulations.

esting to note from Figure 8(a) that it is the cases where the groundwater flow is moderate (2, 3, and 4) that are most over-designed. These cases have peak temperatures of about 74°F (23.3°C), some 16°F (8.9°C) below the maximum design temperature. Considerable drilling cost savings could be seen in cases such as this where shallower borehole depth would have been adequate. It is at higher flows (cases 5 and 6) that the peak temperature is closest to the original design condition after ten years. This illustrates the nonlinearity introduced into the design problem by the presence of advection. It also illustrates the difficulty in adapting conventional design methods to accurately size closed-loop ground heat exchangers in cases of groundwater flow.

The temperature field predicted by the numerical model for case 8 is shown in Figure 9 in the form of a series of contour plots over the ten-year simulation period. These data are plotted for September, as this is when the peak cooling load (i.e., heat rejection to the ground) occurs. The development of the thermal plume over time downstream from the borehole field can be clearly seen. Within the borehole field during the months of heat rejection, the ground temperatures are greatest around the boreholes on the downstream side of the borehole

field. A nearly linear variation in temperature across the borehole field in the direction of flow was found. This suggests that a borehole field wider across the direction of flow and shorter in the direction of flow (e.g., eight rows by two columns in this case) would be advantageous.

A further feature that is shown in the predicted temperature field (Figure 9) is the development of a peak in the ground temperature immediately downstream of the borehole field (approximately 60 m downstream). This arises from the advection downstream of the heat rejected to the ground at the boreholes the previous year. In the contours plotted for year ten, two other peaks can be seen on the centerline of the borehole field further downstream, spaced a similar distance apart but with lower peak temperature. These are associated with the heat rejected in years eight and seven, respectively. This interesting phenomenon arises from the annual cyclic variation in the building loads.

CONCLUSIONS

Using a compilation of “typical” hydraulic and thermal properties of soils and rocks, a preliminary analysis of the effects of groundwater flow on the design and performance of

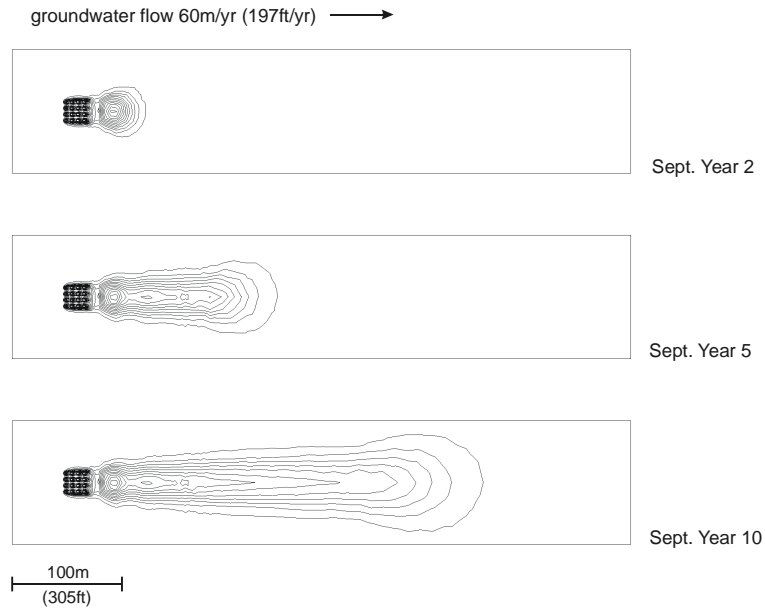


Figure 9 Temperature contours plotted at the end of September for years 2, 5, and 10 for test case 8 showing the development of the thermal plume downstream of the borehole field. The contours are 0.1°C (0.18°F) apart in the range of 17.2°C - 19.2°C (63°F - 66.6°F).

closed-loop ground-coupled heat pump systems has been made. A simple but useful method of assessing the relative importance of heat conduction in the ground vs. heat advection by moving groundwater is demonstrated through the use of the dimensionless Peclet number.

A finite-element numerical groundwater flow and heat transport model was used to simulate and observe the effects of groundwater flow on the heat transfer from a single U-tube closed-loop ground heat exchanger in various geologic materials. From these simulations and from a Peclet number analysis, it appears it is only in geologic material with high hydraulic conductivities, such as coarse-grained soils (e.g., sands and gravels), and in rocks exhibiting secondary porosities, such as fractures and solution channels (e.g., karst limestone), that groundwater flow could be expected to have a significant effect on closed-loop heat exchanger performance.

The effect of groundwater flow on in-situ thermal conductivity test results has been examined by numerically simulating test conditions around a single borehole under different flow conditions. These data were analyzed as if they came from real in-situ sources to arrive at effective thermal conductivity values. As expected, in all cases of groundwater flow, these values were artificially high. Results from one-week test data have been shown to be no more reliable than data from 50-hour tests.

The finite-element numerical groundwater flow and heat transport model was also used to simulate the ten-year performance of borehole fields designed from application of conventional design procedures using the derived thermal

conductivity data. Even very moderate groundwater flows had the effect of removing the year by year increase in ground temperature found in systems where there is no groundwater flow. The borehole fields designed using conventional methods and the derived effective thermal conductivities were generally oversized. However, in some cases at very high groundwater flow rate, temperatures were found to rise above the design criteria.

From this preliminary assessment of the effects of groundwater flow, it appears difficult to adapt results from current design and in-situ measurement methods to fully account for groundwater flow conditions. Over the last decade, considerable progress has been made in developing both in-situ test methods and design procedures for borehole field design for situations where there is no groundwater flow. Research would be required in a number of areas before the same progress could be made to deal with situations of groundwater flow, including:

- Identification of suitable numerical and/or analytical models that include groundwater flow and could be used to analyze in-situ test data.
- Experimental investigation, at sites with significant groundwater flow, of potential in-situ test and data analysis methods.
- Identification of suitable design methods, or adaptations applicable to existing methods, that could be used for closed-loop ground heat exchanger design.
- Development of design guidelines and software tools

that could be used by practicing engineers for in-situ testing and system design tasks in situations of significant groundwater flow.

ACKNOWLEDGEMENTS

This work was supported by the U.S. Department of Energy through contract award DE-FG48-97R810627. Support by the Department of Energy does not constitute endorsement of the views expressed in this article.

NOMENCLATURE

Symbols

ρ	= density (lb/ft ³ [kg/m ³])
c	= specific heat (Btu/lb·°F [J/kg·°C])
D	= diffusion coefficient (ft ² /s [m ² /s])
D^*	= effective thermal diffusivity (ft ² /s [m ² /s])
h	= hydraulic head (ft [m])
k	= thermal conductivity (Btu/h-ft·°F [W/m·°C])
K	= hydraulic conductivity (ft/s [m/s])
L	= characteristic length (ft [m])
n	= porosity (–)
Pe	= Peclet number (–)
Q^*	= heat source/sink term (°F/s [°C/s])
q	= specific discharge (ft/s [m/s])
q^*	= ground thermal load (Btu/h [W])
R	= retardation coefficient (–)
R^*	= groundwater recharge (s ⁻¹ [s ⁻¹])
S_s	= specific storage coefficient (ft ⁻¹ [m ⁻¹])
t	= time (s)
T	= temperature (°F [°C])
v	= average linear groundwater velocity (ft/s [m/s])
V^*	= volumetric flow rate (ft ³ /s [m ³ /s])

Subscripts

eff	= effective
i, j	= coordinate indices
l	= liquid phase
s	= solid phase
w	= injected/extracted water

REFERENCES

- Austin, W.A., C. Yavuzturk, and J. D. Spitler. 2000. Development of an in-situ system for measuring ground thermal properties. Submitted for publication to *ASHRAE Transactions*.
- Bear, J. 1972. *Dynamics of fluids in porous media*. New York: Dover Publications, Inc.
- BLAST. 1986 *BLAST (Building Loads and System Thermodynamics)*. Urbana-Champaign: University of Illinois, BLAST Support Office.
- Carslaw, H.S., and J.C. Jaeger. 1946. *Conduction of heat in solids*. Oxford: Clarendon Press.
- Domenico, P.A., and F.W. Schwartz. 1990. *Physical and chemical hydrogeology*. New York: John Wiley & Sons.
- Driscoll, F.G. 1986. *Groundwater and wells*. St. Paul, Minnesota: Johnson Filtration Systems, Inc.
- Eskilson, P. 1987. *Thermal analysis of heat extraction boreholes*. Doctoral thesis, Lund University, Sweden.
- Eklof, C., and S. Gehlin. 1996. *TED – A mobile equipment for thermal response test*. Master's thesis (1996:198E), Lulea University of Technology, Sweden.
- Fetter, C.W. 1988. *Applied Hydrogeology*. 2d ed. Columbus, Ohio: Merrill Publishing Co.
- Freeze, R.A., and J.A. Cherry. 1979. *Groundwater*. Englewood Cliffs, New Jersey: Prentice-Hall Inc.
- Hellstrom, G. 1991. *Ground heat storage. Thermal Analyses of duct storage systems*. Lund, Sweden: University of Lund, Department of Mathematical Physics.
- IGSHPA. 1991. *Design and installations standards* (Bose, J.E., ed.). Stillwater, Oklahoma: International Ground Source Heat Pump Association.
- Ingersoll, L.R., O.J. Zobel, and A.C. Ingersoll. 1954. *Heat conduction with engineering, geological, and other applications*. New York: McGraw-Hill.
- Kavanaugh, S.P. 1984. *Simulation and experimental verification of vertical ground-coupled heat pump systems*. Ph.D. thesis, Oklahoma State University.
- Kavanaugh, S.P., and K. Rafferty. 1997. *Ground source heat pumps - Design of geothermal systems for commercial and institutional building*. Atlanta: American Society of Heating, Refrigerating and Air-Conditioning Engineers.
- Lindholm, G.F. and J.J. Vaccaro. 1988. (W.B. Back, J.S. Rosenshein, and P.R. Seaber, eds.), Region 2, Columbia lava plateau (Chapter 5). In: *The geology of North America, vol. O-2, hydrogeology*. Boulder, Colo.: The Geological Society of America, Inc.
- Kelvin, Sir W. Thomson. 1882. *Mathematical and physical papers*. vol. II, p.41 ff.
- Mei, V. C. and C.J. Emerson. 1985. New approach for analysis of ground-coil design for applied heat pump systems. *ASHRAE Transactions*, 91 (2B): 1216-1224.
- Mogensen, P. 1983. Fluid to duct wall heat transfer in duct system heat storages. *Proceedings of the International Conference on Subsurface Heat Storage in Theory and Practice*. Swedish council for Building Research, June 6-8, 1983.
- Muraya, N.K., D.L. O'Neal, and W.M. Heffington. 1996. Thermal interference of adjacent legs in a vertical U-tube heat exchanger for a ground-coupled heat pump. *ASHRAE Transactions*, 102 (2): 12-21.
- Remund, C. 1998. Personal communication. Northern Geothermal Support Center, South Dakota State University, Brookings, South Dakota.
- Rottmayer, S.P., W.A. Beckman, and J.W. Mitchell. 1997. Simulation of a single vertical U-tube ground heat

- exchanger in an infinite medium.. *ASHRAE Transactions*, 103 (2): 651-658.
- Shonder, J.A., and J.V. Beck. 1999. Determining effective soil formation thermal properties from field data using a parameter estimation technique. *ASHRAE Transaction*., 105 (1): 458-466.
- Spitler, J.D., C. Marshall, R. Delahoussaye, and M. Manicham. 1996. *Users Guide of GLHEPRO*. Stillwater, OK: School of Mechanical and Aerospace Engineering, Oklahoma State University.
- Stephenson, D.A., A.H. Fleming, and D.M. Mickelson. 1988. (W.B. Back, J.S. Rosenshein, and P.R. Seaber, eds.), Glacial deposits (Chapter 35). In: *The geology of North America, vol. O-2, hydrogeology*. Boulder, Colo.: The Geological Society of America, Inc.
- United States Environmental Protection Agency. 1996. *BIO-SCREEN. Natural attenuation decision support system, user's manual*. Cincinnati, Ohio: National Risk Management Research Laboratory, Office of Research and Development.
- Vatnaskil. 1998. *AQUA3D groundwater flow and contaminant transport model*. Reykjavik, Iceland: Vatnaskil Consulting Engineers.
- Weeks, J.B., and E.D. Gutentag. 1988. (W.B. Back, J.S. Rosenshein, and P.R. Seaber, eds.), Region 17, High plains (Chapter 20). In: *The geology of North America, vol. O-2, hydrogeology*. Boulder, Colo.: The Geological Society of America, Inc.